PLOS ONE

RESEARCH ARTICLE

Pharmaceutical iron formulations do not cross a model of the human blood-brain barrier

Brian Chiou[1], Emma H. Neal[2], Aaron B. Bowman[3,4,5], Ethan S. Lippmann[2,6], Ian A. Simpson[7], James R. Connor[1]*

1 Department of Neurosurgery, Penn State Hershey Medical Center, Hershey, PA, United States of America, **2** Department of Chemical and Biomolecular Engineering, Vanderbilt University, Nashville, TN, United States of America, **3** Department of Pediatrics, Vanderbilt University Medical Center, Nashville, TN, United States of America, **4** Department of Neurology, Vanderbilt University Medical Center, Nashville, TN, United States of America, **5** Department of Biochemistry, Vanderbilt University Medical Center, Nashville, TN, United States of America, **6** Department of Biomedical Engineering, Vanderbilt University, Nashville, TN, United States of America, **7** Department of Neural and Behavioral Sciences, Penn State Hershey Medical Center, Hershey, PA, United States of America

* jconnor@pennstatehealth.psu.edu

Citation: Chiou B, Neal EH, Bowman AB, Lippmann ES, Simpson IA, Connor JR (2018) Pharmaceutical iron formulations do not cross a model of the human blood-brain barrier. PLoS ONE 13(6): e0198775. https://doi.org/10.1371/journal.pone.0198775

Editor: Mária A. Deli, Hungarian Academy of Sciences, HUNGARY

Received: March 6, 2018

Accepted: May 24, 2018

Published: June 11, 2018

Data Availability Statement: All relevant data are within the paper.

Funding: Funding for this study was provided by Luitpold Pharmaceuticals Inc. and NIH R01 NS077678 (JRC). Luitpold Pharmaceuticals Inc. provided support in the form of salaries for author JRC, but did not have any additional role in the study design, data collection, data interpretation, decision to publish, or preparation of the manuscript. Information about Luitpold Pharmaceuticals Inc. can be found at www.luitpold.

Abstract

Whether iron formulations used therapeutically for a variety of conditions involving iron deficiency can deliver iron to the brain is a significant clinical question given the impact that iron loading has on the brain in neurodegenerative diseases. In this study, we examine the ability of 5 pharmaceutical iron formulations that are given intravenously for treatment of iron deficiency to cross an *in vitro* model of the blood-brain barrier. The model uses human brain endothelial cells derived from induced pluripotent stem cells. We report that, compared to the natural iron delivery proteins, transferrin and H-ferritin, the pharmaceutical iron formulations neither cross the blood-brain barrier model nor significantly load the endothelial cells with iron. Furthermore, we report that mimicking brain iron sufficiency or deficiency by exposing the endothelial cells to apo- or holo-transferrin does not alter the amount of iron compound transported by or loaded into the cells. Coupled with previous studies, we propose that pharmaceutical iron formulations must first be processed in macrophages to make iron bioavailable. The results of this study have significant clinical and mechanistic implications for the use of therapeutic iron formulations.

Introduction

Iron is a crucial micronutrient serving as a cofactor in various cellular processes such as myelination, oxygen transport, and DNA synthesis [1]. However, as a transition element, it has properties enabling generation of oxygen free radicals and oxidative stress through the Fenton reaction [2]. As a result, iron levels are tightly regulated because both too much iron as well as a deficiency in iron can be detrimental to biological function and health [3–7].

Iron deficiency (ID) is the most common and widespread nutritional disorder with over 2 billion people suffering significant negative health effects worldwide [8]. In children, ID

com. The hiPSC lines used in this study were developed by funding from National Institutes of Health/National Institute of Environmental Health Sciences RO1 ES016931 (ABB) and RO1 ES010563 (ABB).

Competing interests: I have read the journal's policy and the authors of this manuscript have the following competing interests: JRC is the founder and chairman of the board of Sidero Biosciences LLC, a company with a product involving oral delivery of ferritin for management of iron deficiency. This does not alter our adherence to PLOS ONE policies on sharing data and materials. All other authors have declared that no competing interests exist.

impedes mental and motor development leading to lifelong muscular and cognitive deficiencies [9–11]. In adults, ID leads to extreme fatigue, reduced work capacity and physical performance, hearing loss, recurrent infection, heart failure morbidity, and general reduced quality of life [8,12,13]. There is a widespread, serious misperception that oral iron supplements are safe and effective at alleviating ID. In a recent Cochrane review of 61 clinical trials, women taking oral iron supplements had just a 38% decreased risk of ID at the end of treatment compared to placebo [14].

Intravenous iron delivery is an option for iron supplementation, particularly in persons with conditions such as heavy uterine bleeding or anemia of chronic disease in which oral iron uptake from the gut may be limited due to inflammation. Although intravenous infusion of iron may present a potentially more effective method of iron supplementation [15], concerns exist regarding the safety of intravenous iron delivery [16–19]. One concern is how repeated iron supplementation may impact brain iron load. Although uptake of iron from the blood into the brain is subject to regulation by the blood-brain barrier (BBB), excess iron in the brain is associated with Parkinson's and Alzheimer's disease, amyotrophic lateral sclerosis, and neurodegeneration with brain iron accumulation [20]. Conversely, intravenous iron treatment is under clinical investigation for use in neurological syndromes such as Restless Legs syndrome [21].

Our recent studies have shown that brain iron transport via transferrin is not a simple transcytotic process as once taught [22]. A direct transcytosis model does not account for regulation of iron uptake into the brain nor does it account for the iron requirements of the metabolically active endothelial cells. Thus we proposed a data-based model that reveals iron is released into the cytoplasm of the endothelial cells where it can be stored in ferritin if not immediately used. Moreover, iron can be released from the endothelial cells in response to the ratio of holo- (iron loaded) to apo- (iron poor) transferrin on the brain side of the BBB [22,23]. Therefore, the question of transport of iron into the brain by different chemical formulations must begin with investigation of the potential for transport of iron across the BBB. This study is the first to directly interrogate the ability of various intravenous pharmaceutical iron formulations that are commonly used in the clinic to treat systemic iron deficiency, including Feraheme (ferumoxytol), Venofer (iron sucrose), Dexferrum (iron dextran), Injectafer (ferric carboxymaltose), and Ferrlecit (sodium ferric gluconate) to cross the BBB.

Materials and methods

Human brain endothelial cell culture

Human brain endothelial cells (huECs) were differentiated from CC3 induced pluripotent stem cell (iPSC) lines as previously described [24–28]. Briefly, iPSCs were maintained in E8 medium (prepared in-house) [29] on growth factor reduced Matrigel (Corning) and passaged using Versene (Thermo Fisher Scientific) upon reaching approximately 70% confluence. For differentiation, cells were washed once with DPBS (Thermo Fisher Scientific) and incubated with Accutase (Stem Cell Technologies) for 3 min at 37˚C to yield a single cell suspension, followed by collection via centrifugation. Cell density and viability were measured using a Countess II (Thermo Fisher Scientific) and Trypan Blue stain (Thermo Fisher Scientific), and cells were plated at a density of 15,600 live cells per square centimeter in E8 medium supplemented with 10 μM Rho-associated, coiled-coil containing protein kinase (ROCK) inhibitor Y27632 (R&D Systems). Approximately 24 h after seeding, differentiation was initiated by media change to E6 media (D0) [30]. E6 media was changed every 24 h for 4 days. On day 4 of differentiation, media was changed to human endothelial serum-free media (hESFM, Thermo Fisher Scientific) plus 1% platelet poor platelet derived serum (PDS, Alfa Aesar), collectively

referred to as EC medium, supplemented with 20 ng/mL basic fibroblast growth factor (bFGF, Peprotech) and 10 μM all-trans retinoic acid (RA, Sigma). Media was not changed for 48 h. On day 6 of differentiation, cells were washed once with DPBS and incubated with Accutase at 37˚C until dissociated into an approximately single cell suspension. Cells were collected via centrifugation and resuspended in freeze medium consisting of 60% EC medium containing 20 ng/mL bFGF, 30% fetal bovine serum (Thermo Fisher Scientific), and 10% Hybri-Max DMSO (Sigma), supplemented with 10 μM Y27632 and 10 μM RA [31]. Cells were frozen overnight at -80˚C in an isopropanol-filled freezing container (Thermo Fisher Scientific) before being transferred to long-term storage in liquid nitrogen.

Transwell filters (24-well Costar Transwell, 0.4 μm pore, polyethylene terephthalate, Corning) were coated with a mixture of collagen IV (1 mg/mL, Sigma) and fibronectin (1 mg/mL, Sigma) at a ratio of 5 parts UltraPure H_2O (Thermo Fisher Scientific), 4 parts Collagen IV, and 1 part Fibronectin. A total of 150 μL of this mixture was used to coat the filters overnight at 37˚C. Cryo-preserved huECs were thawed and then plated overnight at a density of 25,000 huECs per Transwell filter in the apical chamber in 150 μL of EC medium supplemented with 10 μM Y27632, 10 μM RA, and 20 ng/mL bFGF. The basal chamber was filled with 600 μL of the same media. The next day, media was changed in both the apical and basal chamber to EC medium supplemented with 10 μM Y27632 but lacking bFGF and RA. The following day, all experiments were performed. At each step, cells were incubated at 37˚C with 5% CO_2.

Protein preparation

Recombinant H-ferritin was prepared as previously described [32]. Briefly, wild-type human H-ferritin containing a poly-His tag was subcloned into the pET30a(+) vector, to be produced in BL21 *Escherichia coli*. Isopropyl-β-D-thio-galactoside (IPTG, Sigma) was used to induce expression. Following induction, bacteria were lysed in a mixture of Bugbuster (Novagen), benzonase nuclease (VWR), bacterial protease inhibitor cocktail (Sigma) and lysozyme (Roche). H-ferritin protein was purified using a nickel column (GE Healthcare Bio-Sciences) according to the manufacturer's instructions. Identity of H-ferritin was verified by western blot (*data not shown*).

Apo-transferrin (apo-Tf, Sigma) and H-ferritin were iron loaded with ferric chloride hexahydrate ($FeCl_3$, Sigma), nitrilotriacetic acid (NTA, Sigma), and sodium bicarbonate complexed at a ratio of 100 μL NTA: 13.4 μL $FeCl_3$: 23.3 μL $NaHCO_3$. This solution was allowed to complex for 30 minutes to create the Fe-NTA complex. Apo-Tf and H-ferritin were incubated with the Fe-NTA complex for 30 additional minutes to allow for sufficient iron loading [22,23].

Transport studies

Prior to the start of the experiment, both the apical and basal chambers were washed with 1X PBS and underwent a complete media exchange into hESFM plus 10 μM Y27632, to remove serum. After media addition, Trans-Endothelial Electrical Resistance (TEER) readings were taken using an Epithelial Volt/Ohm Meter for TEER (EVOM2 with STX2 electrodes, World Precision Instruments) [33]. Blank (media only) TEER values were subtracted from all other TEER measurements. 4.4 kDa TRITC-Dextran (Sigma) was added to the apical chamber at the start of each experiment with the experimental treatment and assayed from the basal chamber (Excitation: 557 nm, Emission: 576 nm) at each timepoint to assess tight junction formation and barrier permeability using a SpectraMax Gemini EM plate reader (Molecular Devices).

At the start of the experiment, 300 μg/mL of each intravenous iron formulation, holo-transferrin (holo-Tf), or H-ferritin was added to the apical chamber. This concentration of iron formulations was chosen as the most clinically relevant concentration and was also informed by

our previous cytotoxicity studies in macrophages [34]. Furthermore, 1 mg/mL apo-Tf or holo-Tf was added to the basal chamber where indicated, doses we have previously used in previous studies by our lab [34]. At 2, 4, 6, 8 and 24 hours, samples were taken from the basal chamber and assayed for TRITC (as a control for any leakage of the tight junctions) signal and iron content. At 24 hours, the endothelial cells were harvested and analyzed for iron content. For all cases, blank (no treatment) controls were subtracted from all other measurements.

Samples (100 μL) at each time point were analyzed for iron content via inductively coupled plasma mass spectrometry (ICP-MS) with Collision Cell Technology (CCT). Prior to analysis, samples were digested in 8 N nitric acid at 60˚C overnight. This solution was diluted to a final concentration of 0.3 N nitric acid and analyzed via ICP-MS (Thermo Fisher Scientific X Series 2). Samples were analyzed by an external calibration method using standards with concentrations ranging between 0 and 100 parts per billion (ppb). Reported measurements of iron in each sample represent the average of 3 measurements.

Statistical analysis

Statistical analysis was performed using Graphpad Prism 4 software (GraphPad Software, Inc.). Data from three technical replicates were averaged and are expressed as the mean ± standard deviation (SD). Two-way ANOVA with Bonferroni *post-hoc* analysis was used where appropriate. A p-value of <0.05 was considered significant.

Results

Using an *in vitro* model of the BBB, we first examined the ability of transferrin, H-ferritin, or the iron formulations to promote iron transport across the huECs. Transferrin and H-ferritin were included in the experiment as positive controls because previous studies have shown transport of both of these proteins [22,23,35], while untreated cells were used to establish baseline measurements (Fig 1). A 4.4 kDa TRITC-Dextran complex was included as a readout for barrier permeability; <0.5% leakage was observed. Furthermore, TEER values from this experiment averaged 1939 ± 314 Ohms x cm^2 across all wells. These values are much greater than our previous studies using primary cells and in line with previous studies with these cells [22,23,27]. The total iron transport at 24 hours for each of five iron formulations represented less than 0.02% of the total iron formulation (Fig 1). Of the five compounds, Dexferrum was associated with the highest amount of iron observed in the basal chamber (44.13 ng/mL); but this represented only 0.015% of the total Dexferrum initially added to the apical chamber. In comparison, transferrin (127.71 ng/mL) and H-ferritin (1011.9 ng/mL) transported significantly more iron across the huECs at 24 hours ($p<0.001$), representing 9% and 10% of the total exposure respectively.

We have previously established that the iron status of Tf in the basal chamber of the BBB model can signal to the endothelial cells and significantly influence the amount of iron that is transported across or released from the BBB model [22,23]. We added either 1 mg/mL apo-Tf or holo-Tf to the basal chamber of the Transwell bichamber model at the start of the experiment. Apo-Tf significantly increased the amount of iron transported from both transferrin and H-ferritin whereas the addition of holo-Tf decreased the total amount of iron transported for both proteins (Fig 2). In the case of transferrin, the highest amount of iron transported at 24 hours was in the apo-Tf condition (281.9 ± 84.9 ng/mL), while H-ferritin + apo-Tf in the basal chamber (1833.0 ± 451.2 ng/mL) represented the highest overall transport of iron across all conditions (Table 1). There was no significant change in the amount of iron transported for any of the iron formulations in the presence of either apo- or holo-Tf in the basal chamber.

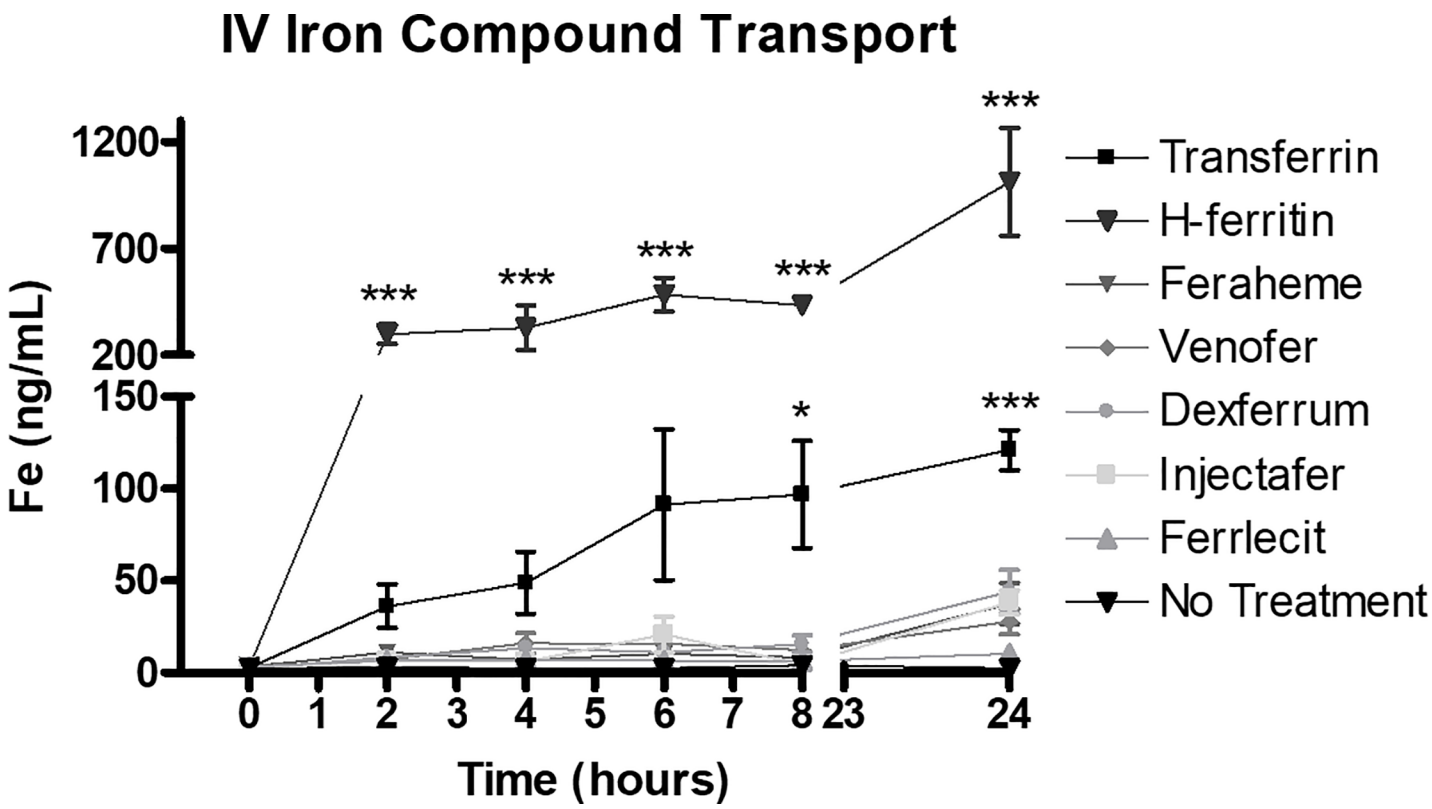

Fig 1. Commercial iron formulations do not transport iron across a BBB model. Using the bichamber model of the BBB, H-ferritin and Tf robustly transport iron across the huECs at each time point. Minimal iron transport is observed for the 5 commercial iron formulations. The concentration of the commercial formulations, Tf and H-ferritin was 300 μg/ml. All values are means ± SD, with statistical significance evaluated against the untreated control using two-way ANOVA and Bonferroni's *post hoc* comparisons. * = $p<0.05$, *** = $p<0.001$.

https://doi.org/10.1371/journal.pone.0198775.g001

Moreover, even with the addition of apo-Tf or holo-Tf, total percent iron transport still did not exceed 0.02% of the initial addition (Table 1).

We also found that the iron formulations do not load the huECs with iron. We compared the iron loading of huECs by the 5 IV iron formulations, Tf, and Hft across three conditions: a control condition that had no Tf added to the basal chamber and two experimental conditions where 1 mg/mL apo-Tf or holo-Tf was added to the basal chamber media. The addition of apo- or holo-Tf to the basal media failed to significantly increase iron loading of the cells by the iron formulations (Table 2). In contrast, both Tf and Hft significantly increased the iron content of the huECs over control. Moreover, the addition of apo-Tf to the basal chamber increased the iron content of the huECs by 50.4% for iron loading by Tf and 87.6% for Hft whereas the presence of holo-Tf in the basal chamber decreased iron loading by Tf by 22.9% and 54.0% by Hft ($p<0.001$ for all values). In these experiments, the total amount of TRITC--Dextran leakage observed was <0.5%. The TEER values across all conditions averaged 1728 ± 424 Ohms x cm^2.

Discussion

The development of therapeutic iron compounds that can be given intravenously represents a potentially effective and rapid method for the treatment of iron deficiency. The results of this study demonstrate that there is no inherent ability of these pharmaceutical iron formulations to be taken up by the human brain endothelial cells or for the iron to be transported across the

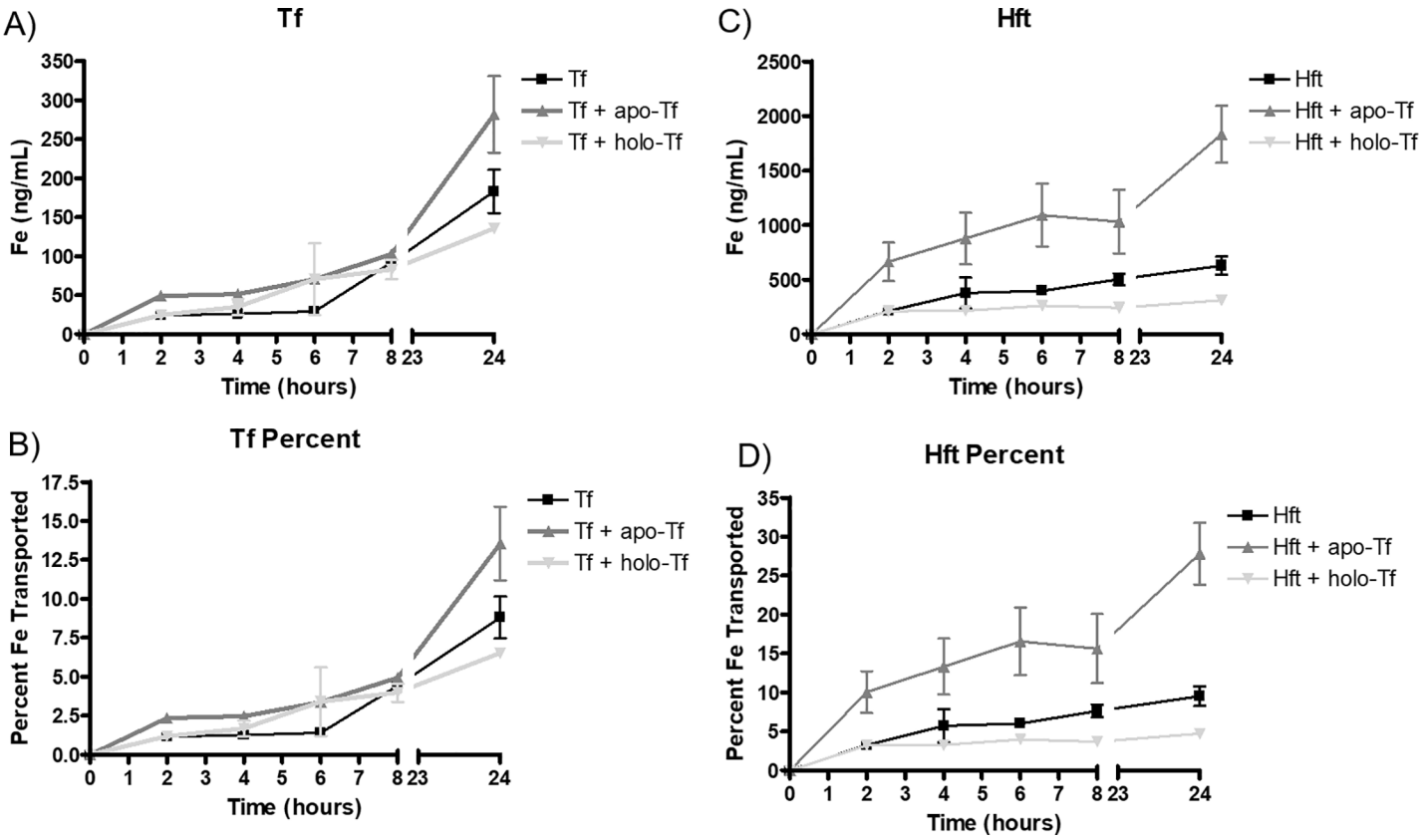

Fig 2. Transferrin and H-ferritin transport of iron is responsive to signaling by apo- and holo-Tf. A) Apo-Tf in the basal chamber increases the amount of iron transported across the endothelial cells by transferrin whereas holo-Tf decreases the amount transported. The control condition is the basal media with no extra addition. **B)** Here, the data from panel A are shown as a percent of control. **C)** Apo-Tf in the basal chamber significantly increases the amount of iron transported by H-ferritin while holo-Tf decreases the amount transported relative to control. **D)** H-ferritin transport of iron from panel C as a percent of control conditions. All values are means ± SD, with statistical significance evaluated against the control (addition of Tf or Hft alone) using two-way ANOVA and Bonferroni's *post hoc* comparisons. * = $p<0.05$, *** = $p<0.001$.

https://doi.org/10.1371/journal.pone.0198775.g002

cells and released. The addition of a stimulus such as apo-Tf, which has been shown in our model to increase iron transport and release [22,23] and confirmed in this study to occur in human brain endothelial cells, had no impact on the iron formulations. The ability of apo-Tf and holo-Tf to alter iron transport and release has been posited by our group to represent signaling regarding brain iron status and to account for local iron regulation in the brain [23].

In this study, we used human brain endothelial cells that have been differentiated from iPSCs [26] to examine the ability of 5 iron formulations to be transported in a novel *in vitro* BBB model. Transferrin and H-ferritin are established as natural iron delivery proteins and thus served as positive controls [33]. Here, we demonstrate that the addition of the various iron formulations resulted in less than 0.02% iron transport across the BBB, even in the presence of apo-Tf. In comparison, both transferrin and H-ferritin robustly transported iron. Furthermore, we demonstrate that 24 hour exposure to these pharmaceutical iron formulations does not result in iron loading of the human endothelial cells. Tthe corresponding exposure to Hft or Tf for the same time resulted in significant iron loading. These results are consistent with our reports on bovine microvasculature BBB models [23] and microvasculature from human brain that endothelial cells of the BBB load iron and can serve as an iron reservoir [36].

Given that the pharmaceutical iron formulations did not load the endothelial cells with iron begs the question of how the iron in these formulations becomes bioavailable. It is generally

Table 1. Transport of iron across the BBB.

	Time (hours)				
Treatment	**2**	**4**	**6**	**8**	**24**
	Iron Values Reported as ng/mL				
Transferrin	24.2 ± 2.0	26.2 ± 1.7	29.2 ± 8.6	92.0 ± 8.5	183.2 ± 48.3
Tf + apo-Tf	49.1 ± 3.9	51.4 ± 5.9	70.3 ± 10.1	102.7 ± 11.8	281.9 ± 84.9**
Tf + holo-Tf	24.7 ± 0.9	35.2 ± 17.6	70.7 ± 19.2	82.9 ± 21.3	135.7 ± 11.4
H-Ferritin	214.1 ± 10.4	377.7 ± 24.4	397.5 ± 37.0	503.5 ± 91.0	628.1 ± 144.2
Hft + apo-Tf	662.8 ± 204.4	877.2 ± 309.3	1091.1 ± 296.6	1030.4 ± 305.1	1833.0 ± 451.2**
Hft + holo-Tf	212.0 ± 12.9	215.4 ± 19.2	261.9 ± 22.7	242.3 ± 12.9	311.9 ± 29.5
Feraheme	9.4 ± 0.2	12.0 ± 1.0	8.4 ± 0.3	11.1 ± 3.3	8.4 ± 0.5
Feraheme + apo-Tf	9.2 ± 0.7	15.9 ± 0.2	11.3 ± 5.2	22.7 ± 2.1	21.4 ± 15.9
Feraheme + holo-Tf	11.5 ± 2.7	17.9 ± 4.5	12.3 ± 5.6	18.2 ± 3.6	9.2 ± 2.0
Venofer	9.9 ± 2.7	18.3 ± 9.7	13.2 ± 3.4	20.1 ± 8.4	13.7 ± 4.7
Venofer + apo-Tf	7.8 ± 5.2	9.2 ± 1.6	4.8 ± 0.3	8.5 ± 1.7	6.2 ± 0.1
Venofer + holo-Tf	15.5 ± 2.5	17.6 ± 3.4	17.9 ± 3.2	20.8 ± 7.3	18.9 ± 5.0
Dexferrum	13.1 ± 3.5	19.7 ± 8.1	19.0 ± 6.6	33.5 ± 19.6	46.1 ± 22.1
Dexferrum + apo-Tf	20.5 ± 14.4	23.1 ± 9.3	20.2 ± 4.2	19.8 ± 7.9	22.2 ± 4.6
Dexferrum + holo-Tf	10.1 ± 1.9	11.3 ± 4.8	16.1 ± 3.1	15.8 ± 8.2	19.1 ± 6.6
Injectafer	8.5 ± 2.0	5.0 ± 0.6	19.8 ± 9.4	8.5 ± 4.1	34.9 ± 10.4
Injectafer + apo-Tf	12.5 ± 4.4	12.1 ± 4.3	19.8 ± 9.0	11.8 ± 3.8	47.5 ± 20.0
Injectafer + holo-Tf	8.4 ± 6.8	13.6 ± 11.9	5.5 ± 0.4	20.1 ± 2.2	5.9 ± 1.0
Ferrlecit	13.5 ± 2.2	19.4 ± 4.3	16.4 ± 2.3	13.6 ± 2.4	27.7 ± 17.8
Ferrlecit + apo-Tf	5.3 ± 0.6	6.3 ± 1.0	5.0 ± 0.4	9.6 ± 1.7	27.3 ± 2.3
Ferrlecit + holo-Tf	11.3 ± 7.9	16.5 ± 2.7	15.0 ± 5.2	13.7 ± 1.1	16.2 ± 10.7

Presented here are the raw values of iron transport in ng/mL at times 2, 4, 6, 8, and 24 hours post addition of iron formulations to the apical chamber. Apo-Tf significantly increased the amount of Tf and Hft bound iron transported, but did not affect transport of the iron formulations. All values are means ± SD, statistical significance evaluated against the control (addition of Tf or Hft alone at 24 hours) using two-way ANOVA and Bonferroni's *post hoc* comparisons.

** = $p<0.01$.

https://doi.org/10.1371/journal.pone.0198775.t001

Table 2. Iron loading of endothelial cells.

	Control (ng/mL)	+apo-Tf (ng/mL)	+holo-Tf (ng/mL)
Transferrin	580.9 ± 121.7	874.0 ± 49.5***	448.1 ± 11.8***
H-ferritin	1176.9 ± 304.1	2207.3 ± 170.6***	541.6 ± 87.3***
Feraheme	22.0 ± 2.7	24.8 ± 3.7	6.3 ± 0.2
Venofer	92.9 ± 11.2	19.4 ± 2.1	98.9 ± 1.8
Dexferrum	31.0 ± 10.6	29.1 ± 5.0	22.5 ± 5.8
Injectafer	31.5 ± 3.2	30.0 ± 4.9	41.0 ± 4.2
Ferrlecit	75.3 ± 2.2	75.1 ± 9.3	65.9 ± 13.8
No Treatment	5.9 ± 0.8	7.2 ± 2.5	5.2 ± 0.7

After 24 hours of exposure to the different iron formulations, endothelial cells were harvested and their iron content determined by ICP-MS, presented here as ng/mL. There was iron loading by the different formulations compared to control (no treatment). However, this iron loading was much less compared to loading by Tf or Hft. All values are means ± SD, statistical significance evaluated against the control (addition of Tf or Hft alone) using two-way ANOVA and Bonferroni's *post hoc* comparisons.

*** = $p<0.001$.

https://doi.org/10.1371/journal.pone.0198775.t002

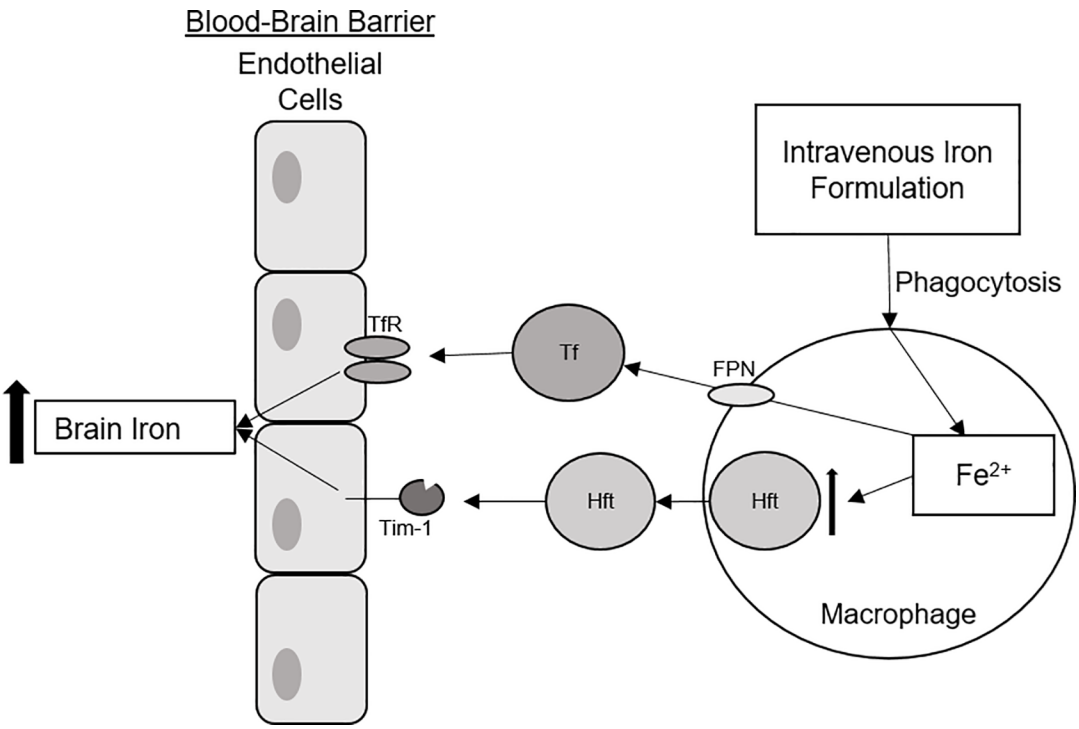

Fig 3. Schematic representation of hypothesized route of IV iron compound after administration. After the IV iron formulations are administered, they are may be initially picked up by macrophages. The macrophages proceed to metabolize the IV iron formulations, storing the excess iron in H-ferritin (Hft). Additionally, free iron may be exported from the macrophage via ferroportin (FPN) where it may be picked up by circulating apo-transferrin or ferritin. Transferrin (Tf) or Hft can bind to transferrin receptor (TfR) or the T-cell immunoglobulin and mucin domain 1 (Tim-1) receptor [42], and then provide iron across the BBB as demonstrated in this study.

https://doi.org/10.1371/journal.pone.0198775.g003

accepted that the reticular endothelial cell system may be the first cells to accumulate iron from the iron formulations. In this paradigm, macrophages are a key component of this system and the innate immune response, serving to phagocytose foreign antigens, such as circulating drugs [37,38]. We have reported that peripheral macrophages take up the iron formulations in a cell culture model [34]. Additionally, after internalizing the iron formulations, macrophages increase release of Hft and exported free iron through ferroportin, the only known iron exporter [34]. The iron released through ferroportin would be available to bind to Tf. Indeed, when macrophages are incubated with apo-Tf in the media, they increase their iron release [39] similar to what we have reported and demonstrated herein for endothelial cells. Hepcidin, an iron regulatory hormone released by hepatocytes, was shown to block ferroportin release of iron [40]. Thus, we posit that macrophages could represent a key intermediary for making iron from the pharmaceutical formulations available bound to Hft or Tf for regulated (receptor mediated) uptake into the brain and other organs (Fig 3). It should be noted that macrophages also are key players in the iron-withholding defense mechanism during inflammation; a process mediated by hepcidin [40,41].

Pharmaceutical iron formulations have been tested clinically for treatment of neurological disorders such as Restless Legs syndrome (RLS) and have also been used as a potential contrast agent in imaging brain tumors [43,44]. Our data would suggest that for brain tumor imaging the iron compounds can only penetrate through areas where the BBB is compromised similar to the gadolinium based compounds and then accumulate in macrophages within the tumor [45,46]. In a study to determine if an IV iron compound (Monofer, iron isomaltoside-1000)

can enter the brain, Unger et al. demonstrated regional correction of iron deficiency in the brain in a rodent model following a tail vein injection of iron isomaltoside-1000 [47]. This correction was observed without producing iron overload in any of the brain regions whose iron status was unchanged by the iron deficiency. Using microdialysis to detect iron in the brain, they reported a transient increase in iron uptake and that the iron was not Tf-bound. Although we did not include iron isomaltoside-1000 in our study, the regional uptake of iron observed by Unger et al. is in agreement with our findings that the pharmaceutical formulations do not cross the BBB. If iron isomaltoside-1000 natively passed through the BBB, systemic administration of iron isomaltoside-1000 it should have produced whole brain iron uptake, but only regional uptake was observed. Thus, the compound that was delivered via tail vein, may have first passed through the macrophage system as we have suggested (Fig 3).

Overall, this study serves to guide clinical treatment plans using pharmaceutical-grade intravenous iron formulations. Because the data presented herein suggest that iron formulations themselves do not directly cross the BBB, concerns that brain iron overload could result from IV iron treatments may be mitigated; albeit within the caveats associated with extrapolation from in vitro models. For treatments that are designed to alleviate symptoms of neurological disorders such as RLS, our data suggest that iron made available to the brain may first require processing in cells such as macrophages and then is subject to processes in place to regulate brain iron uptake.

Acknowledgments

The authors thank Matthew Gonzales from the Penn State Laboratory for Isotopes and Metals in the Environment for assistance with ICP-MS.

Author Contributions

Conceptualization: Brian Chiou, Ian A. Simpson, James R. Connor.

Data curation: Brian Chiou, James R. Connor.

Formal analysis: Brian Chiou, Ian A. Simpson, James R. Connor.

Funding acquisition: James R. Connor.

Investigation: Brian Chiou.

Resources: Emma H. Neal, Aaron B. Bowman, Ethan S. Lippmann, James R. Connor.

Supervision: James R. Connor.

Validation: Brian Chiou.

Writing – original draft: Brian Chiou, Emma H. Neal, Aaron B. Bowman, Ethan S. Lippmann, Ian A. Simpson, James R. Connor.

Writing – review & editing: Brian Chiou, Emma H. Neal, Aaron B. Bowman, Ethan S. Lippmann, Ian A. Simpson, James R. Connor.

References

1. Beard JL, Dawson H, Piñero DJ. Iron metabolism: a comprehensive review. Nutr Rev. 1996; 54: 295–317. PMID: 9063021
2. Arosio P, Ingrassia R, Cavadini P. Ferritins: A family of molecules for iron storage, antioxidation and more. Biochim Biophys Acta—Gen Subj. 2009; 1790: 589–599. https://doi.org/10.1016/j.bbagen.2008.09.004 PMID: 18929623

3. Peters DG, Connor JR, Meadowcroft MD. The relationship between iron dyshomeostasis and amyloidogenesis in Alzheimer's disease: Two sides of the same coin. Neurobiol Dis. Elsevier Inc.; 2015; 81: 49–65. https://doi.org/10.1016/j.nbd.2015.08.007 PMID: 26303889
4. Burdo J., Antonetti D., Wolpert E., Connor J. Mechanisms and regulation of transferrin and iron transport in a model blood–brain barrier system. Neuroscience. 2003; 121: 883–890. https://doi.org/10.1016/S0306-4522(03)00590-6 PMID: 14580938
5. Shpyleva SI, Tryndyak VP, Kovalchuk O, Starlard-Davenport A, Chekhun VF, Beland FA, et al. Role of ferritin alterations in human breast cancer cells. Breast Cancer Res Treat. 2011; 126: 63–71. https://doi.org/10.1007/s10549-010-0849-4 PMID: 20390345
6. Grishchuk Y, Pena KA, Coblentz J, King VE, Humphrey DM, Wang SL, et al. Impaired myelination and reduced brain ferric iron in the mouse model of mucolipidosis IV. Dis Model Mech. 2015; 8: 1591–1601. https://doi.org/10.1242/dmm.021154 PMID: 26398942
7. Hametner S, Wimmer I, Haider L, Pfeifenbring S, Brück W, Lassmann H. Iron and neurodegeneration in the multiple sclerosis brain. Ann Neurol. 2013; 74: 848–861. https://doi.org/10.1002/ana.23974 PMID: 23868451
8. Zimmermann MB, Hurrell RF. Nutritional iron deficiency. Lancet. 2007. pp. 511–520. https://doi.org/10.1016/S0140-6736(07)61235-5 PMID: 17693180
9. Sun AH, Xiao SZ, Li BS, Li ZJ, Wang TY, Zhang YS. Iron deficiency and hearing loss. Experimental study in growing rats. ORL J Otorhinolaryngol Relat Spec. 1987; 49: 118–122. https://doi.org/10.1159/000275920 PMID: 3614852
10. Cortese S, Angriman M, Lecendreux M, Konofal E. Iron and attention deficit/hyperactivity disorder: what is the empirical evidence so far? A systematic review of the literature. Expert Rev Neurother. 2012; 12: 1227–1240. https://doi.org/10.1586/ern.12.116 PMID: 23082739
11. Reynolds A, Krebs NF, Stewart PA, Austin H, Johnson SL, Withrow N, et al. Iron Status in Children With Autism Spectrum Disorder. Pediatrics. 2012; 130: S154–S159. https://doi.org/10.1542/peds.2012-0900M PMID: 23118246
12. Cohen-Solal A, Leclercq C, Deray G, Lasocki S, Zambrowski J-J, Mebazaa A, et al. Iron deficiency: an emerging therapeutic target in heart failure. Heart. 2014; 100: 1414–1420. https://doi.org/10.1136/heartjnl-2014-305669 PMID: 24957529
13. Camaschella C. Iron deficiency: new insights into diagnosis and treatment. Hematology. 2015; 2015: 8–13. https://doi.org/10.1182/asheducation-2015.1.8 PMID: 26637694
14. Peña-Rosas JP, De-Regil LM, Garcia-Casal MN, Dowswell T. Daily oral iron supplementation during pregnancy. In: Peña-Rosas JP, editor. Cochrane Database of Systematic Reviews. Chichester, UK: John Wiley & Sons, Ltd; 2015. p. Art. No.: CD004736. https://doi.org/10.1002/14651858.CD004736.pub5 PMID: 26198451
15. Cho YW, Allen RP, Earley CJ. Lower molecular weight intravenous iron dextran for restless legs syndrome. Sleep Med. 2013; 14: 274–277. https://doi.org/10.1016/j.sleep.2012.11.001 PMID: 23333678
16. Kim BJ, Lee SH, Koh JM, Kim GS. The association between higher serum ferritin level and lower bone mineral density is prominent in women ≥45 years of age (KNHANES 2008–2010). Osteoporos Int. 2013; 24: 2627–2637. https://doi.org/10.1007/s00198-013-2363-0 PMID: 23592044
17. Tsay J, Yang Z, Ross FP, Cunningham-Rundles S, Lin H, Coleman R, et al. Bone loss caused by iron overload in a murine model: Importance of oxidative stress. Blood. American Society of Hematology; 2010; 116: 2582–2589. https://doi.org/10.1182/blood-2009-12-260083 PMID: 20554970
18. Nakchbandi IA. Osteoporosis and fractures in liver disease: Relevance, pathogenesis and therapeutic implications. World Journal of Gastroenterology. 2014. pp. 9427–9438. https://doi.org/10.3748/wjg.v20.i28.9427 PMID: 25071337
19. Kalra PA, Bhandari S. Safety of intravenous iron use in chronic kidney disease. Curr Opin Nephrol Hypertens. 2016; 25: 529–535. https://doi.org/10.1097/MNH.0000000000000263 PMID: 27557350
20. Hagemeier J, Geurts JJ, Zivadinov R. Brain iron accumulation in aging and neurodegenerative disorders. Expert Rev Neurother. 2012; 12: 1467–1480. https://doi.org/10.1586/ern.12.128 PMID: 23237353
21. Allen RP, Picchietti DL, Auerbach M, Cho YW, Connor JR, Earley CJ, et al. Evidence-based and consensus clinical practice guidelines for the iron treatment of restless legs syndrome/Willis-Ekbom disease in adults and children: An IRLSSG task force report. Sleep Med. 2017; https://doi.org/10.1016/j.sleep.2017.11.1126 PMID: 29425576
22. Simpson IA, Ponnuru P, Klinger ME, Myers RL, Devraj K, Coe CL, et al. A Novel Model for Brain Iron Uptake: Introducing the Concept of Regulation. J Cereb Blood Flow Metab. Nature Publishing Group; 2015; 35: 48–57. https://doi.org/10.1038/jcbfm.2014.168 PMID: 25315861

23. Duck KA, Simpson IA, Connor JR. Regulatory mechanisms for iron transport across the blood-brain barrier. Biochem Biophys Res Commun. 2017; 494: 70–75. https://doi.org/10.1016/j.bbrc.2017.10.083 PMID: 29054412

24. Lippmann ES, Azarin SM, Kay JE, Nessler RA, Wilson HK, Al-Ahmad A, et al. Derivation of blood-brain barrier endothelial cells from human pluripotent stem cells. Nat Biotechnol. 2012; 30: 783–791. https://doi.org/10.1038/nbt.2247 PMID: 22729031

25. Lippmann ES, Al-Ahmad A, Palecek SP, Shusta E V. Modeling the blood–brain barrier using stem cell sources. Fluids Barriers CNS. 2013; 10: 2. https://doi.org/10.1186/2045-8118-10-2 PMID: 23305164

26. Lippmann ES, Al-Ahmad A, Azarin SM, Palecek SP, Shusta E V. A retinoic acid-enhanced, multicellular human blood-brain barrier model derived from stem cell sources. Sci Rep. 2014; 4: 1–10. https://doi.org/10.1038/srep04160 PMID: 24561821

27. Hollmann EK, Bailey AK, Potharazu A V, Neely MD, Bowman AB, Lippmann ES. Accelerated differentiation of human induced pluripotent stem cells to blood–brain barrier endothelial cells. Fluids Barriers CNS. 2017; 14: 9. https://doi.org/10.1186/s12987-017-0059-0 PMID: 28407791

28. Kumar KK, Lowe EW, Aboud AA, Neely MD, Redha R, Bauer JA, et al. Cellular manganese content is developmentally regulated in human dopaminergic neurons. Sci Rep. 2015; 4: 6801. https://doi.org/10.1038/srep06801 PMID: 25348053

29. Chen G, Gulbranson DR, Hou Z, Bolin JM, Ruotti V, Probasco MD, et al. Chemically defined conditions for human iPSC derivation and culture. Nat Methods. 2011; 8: 424–429. https://doi.org/10.1038/nmeth.1593 PMID: 21478862

30. Lippmann ES, Estevez-Silva MC, Ashton RS. Defined human pluripotent stem cell culture enables highly efficient neuroepithelium derivation without small molecule inhibitors. Stem Cells. 2014; 32: 1032–42. https://doi.org/10.1002/stem.1622 PMID: 24357014

31. Wilson HK, Faubion MG, Hjortness MK, Palecek SP, Shusta E V. Cryopreservation of Brain Endothelial Cells Derived from Human Induced Pluripotent Stem Cells Is Enhanced by Rho-Associated Coiled Coil-Containing Kinase Inhibition. Tissue Eng Part C Methods. 2016; 22: 1085–1094. https://doi.org/10.1089/ten.tec.2016.0345 PMID: 27846787

32. Todorich B, Zhang X, Connor JR. H-ferritin is the major source of iron for oligodendrocytes. Glia. 2011; 59: 927–935. https://doi.org/10.1002/glia.21164 PMID: 21446040

33. Srinivasan B, Kolli AR, Esch MB, Abaci HE, Shuler ML, Hickman JJ. TEER Measurement Techniques for In Vitro Barrier Model Systems. J Lab Autom. 2015; 20: 107–126. https://doi.org/10.1177/2211068214561025 PMID: 25586998

34. Connor JR, Zhang X, Nixon AM, Webb B, Perno JR. Comparative evaluation of nephrotoxicity and management by macrophages of intravenous pharmaceutical iron formulations. Pantopoulos K, editor. PLoS One. 2015; 10: e0125272. https://doi.org/10.1371/journal.pone.0125272 PMID: 25973894

35. Fisher J, Devraj K, Ingram J, Slagle-Webb B, Madhankumar AB, Liu X, et al. Ferritin: a novel mechanism for delivery of iron to the brain and other organs. Am J Physiol Cell Physiol. 2007; 293: C641–9. https://doi.org/10.1152/ajpcell.00599.2006 PMID: 17459943

36. Connor JR, Menzies SL, St. Martin SM, Mufson EJ. A histochemical study of iron, transferrin, and ferritin in Alzheimer's diseased brains. J Neurosci Res. 1992; 31: 75–83. https://doi.org/10.1002/jnr.490310111 PMID: 1613823

37. Lameijer MA, Tang J, Nahrendorf M, Beelen RHJ, Mulder WJM. Monocytes and macrophages as nanomedicinal targets for improved diagnosis and treatment of disease. Expert Rev Mol Diagn. 2013; 13: 567–580. https://doi.org/10.1586/14737159.2013.819216 PMID: 23895127

38. Gustafson HH, Holt-Casper D, Grainger DW, Ghandehari H. Nanoparticle uptake: The phagocyte problem. Nano Today. 2015; 10: 487–510. https://doi.org/10.1016/j.nantod.2015.06.006 PMID: 26640510

39. Nixon AM, Neely E, Simpson IA, Connor JR. The role of HFE genotype in macrophage phenotype. J Neuroinflammation. 2018; 15: 30. https://doi.org/10.1186/s12974-018-1057-0 PMID: 29391061

40. Ganz T. Hepcidin and Its Role in Regulating Systemic Iron Metabolism. Hematology. 2006; 2006: 29–35. https://doi.org/10.1182/asheducation-2006.1.29 PMID: 17124036

41. Ganz T. Macrophages and Iron Metabolism. Microbiol Spectr. 2016; 4. https://doi.org/10.1128/microbiolspec.MCHD-0037-2016 PMID: 27763254

42. Chiou B, Lucassen E, Sather M, Kallianpur A, Connor J. Semaphorin4A and H-ferritin utilize Tim-1 on human oligodendrocytes: A novel neuro-immune axis. Glia. 2018; 1–14. https://doi.org/10.1002/glia.23313 PMID: 29457657

43. Pouliquen D, Le Jeune JJ, Perdrisot R, Ermias A, Jallet P. Iron oxide nanoparticles for use as an MRI contrast agent: Pharmacokinetics and metabolism. Magn Reson Imaging. 1991; 9: 275–283. https://doi.org/10.1016/0730-725X(91)90412-F PMID: 1881245

44. Briley-Saebo K, Bjørnerud A, Grant D, Ahlstrom H, Berg T, Kindberg GM. Hepatic cellular distribution and degradation of iron oxide nanoparticles following single intravenous injection in rats: Implications for magnetic resonance imaging. Cell Tissue Res. 2004; 316: 315–323. https://doi.org/10.1007/s00441-004-0884-8 PMID: 15103550

45. Etheridge ML, Campbell SA, Erdman AG, Haynes CL, Wolf SM, McCullough J. The big picture on nanomedicine: the state of investigational and approved nanomedicine products. Nanomedicine Nanotechnology, Biol Med. 2013; 9: 1–14. https://doi.org/10.1016/j.nano.2012.05.013 PMID: 22684017

46. Albrecht DS, Granziera C, Hooker JM, Loggia ML. In Vivo Imaging of Human Neuroinflammation. ACS Chem Neurosci. 2016; 7: 470–483. https://doi.org/10.1021/acschemneuro.6b00056 PMID: 26985861

47. Unger EL, Earley CJ, Thomsen LL, Jones BC, Allen RP. Effects of IV iron isomaltoside-1000 treatment on regional brain iron status in an iron-deficient animal. Neuroscience. 2013; 246: 179–185. https://doi.org/10.1016/j.neuroscience.2013.04.049 PMID: 23660192